

# The ‘Friction’ of Vacuum, and other Fluctuation–Induced Forces

Mehran Kardar

*Department of Physics, Massachusetts Institute of Technology, Cambridge, MA 02139*

Ramin Golestanian

*Institute for Advanced Studies in Basic Sciences, Zanjan 45195-159, Iran*

(December 2, 2024)

The *static* Casimir effect describes an attractive force between two conducting plates, due to *quantum fluctuations* of the electromagnetic (EM) field in the intervening space. *Thermal fluctuations* of correlated fluids (such as critical mixtures, super-fluids, or liquid crystals) are also modified by the boundaries, resulting in finite-size corrections at criticality, and additional forces that effect wetting and layering phenomena. Modified fluctuations of the EM field can also account for the ‘van der Waals’ interaction between conducting spheres, and have analogs in the fluctuation–induced interactions between inclusions on a membrane. We employ a path integral formalism to study these phenomena for boundaries of arbitrary shape. This allows us to examine the many unexpected phenomena of the *dynamic* Casimir effect due to moving boundaries. With the inclusion of quantum fluctuations, the EM vacuum behaves essentially as a complex fluid, and modifies the motion of objects through it. In particular, from the mechanical response function of the EM vacuum, we extract a plethora of interesting results, the most notable being: **(i)** The effective mass of a plate depends on its shape, and becomes anisotropic. **(ii)** There is dissipation and damping of the motion, again dependent upon shape, and direction of motion. **(iii)** There is a continuous spectrum of resonant cavity modes that can be excited by the motion.

## I. FLUCTUATION–INDUCED FORCES

The standard Casimir effect [1] is a macroscopic manifestation of quantum fluctuations of vacuum. In 1948, Casimir considered the electromagnetic field in the cavity formed by two conducting plates at a separation  $H$ . Because the electric field must vanish at the boundaries, the normal modes of the cavity are characterized by wave-vectors  $\vec{k} = (k_x, k_y, \pi n/H)$ , with integer  $n$ . Once quantized, these normal modes can be regarded as harmonic oscillators of frequencies  $\omega(\vec{k}) = c|\vec{k}|$ ; each of which in its ground state has energy  $\hbar\omega(\vec{k})/2$ . While adding up all the ground state energies leads to an infinite contribution to the overall energy  $\mathcal{E}(H)$ , Casimir showed that the a finite *attractive* force is obtained from

$$F(H) = -\frac{\partial\mathcal{E}}{\partial H} = -\hbar c \times \frac{A}{H^4} \times \frac{\pi^2}{240}, \quad (1)$$

where  $A$  is the area of the plates. Thus, by measuring the mechanical force between macroscopic bodies, it is in principle possible to gain information about the behavior of the quantum vacuum.

The predictions of Casimir were followed by experiments on quartz [2] and aluminum [3] plates at separations  $H > 10^3\text{\AA}$ . However, these experiments, and others reviewed in Ref. [4], provided results that were at best in qualitative agreement with Eq.(1). It is only quite recently that high precision measurements of the force (using a torsion pendulum) between a gold plate, and gold plated sphere, confirmed the accuracy of the theoretical prediction to within %5 [5].

While the Casimir interaction is due to the *quantum fluctuations* of the electromagnetic field, there are several examples in *classical statistical mechanics*, where forces are induced by the *thermal fluctuations* of a correlated fluid. One of the best known examples comes from the finite size corrections to the free energy at a critical point [6]. As demonstrated originally by Fisher and de Gennes [7], there is a contribution to the free energy of a critical film, that varies with its thickness  $H$ , as

$$\delta\mathcal{F}(H) = -k_B T \times \frac{A}{H^2} \times \Delta. \quad (2)$$

This is to be expected on dimensional grounds, as the free energy comes from thermal fluctuations, hence proportional to  $k_B T$ , and must be extensive. (Similar analysis in  $d$ -dimensions leads to a dependence as  $1/H^{d-1}$ .) The dimensionless amplitude  $\Delta$  is closely related to the so called central charge of the critical theory, and in two dimensions exact values can be obtained by employing techniques of conformal field theories [8]. In higher dimensions, they can be estimated numerically [9], and by  $\epsilon = 4 - d$  expansions [10].

Equation (2) results in a force that decays as  $1/H^3$ . The difference in the power of  $H$  from Eq.(1) is that the fluctuation energy in the latter is quantum in origin, hence proportional to  $\hbar c$ , which has dimensions of *energy times length*.

In fact, long-range forces are induced by thermal fluctuations of any *correlated medium*, by which we mean any system with fluctuations that have long-range correlations. A critical system is a very particular example; much more common are cases where long-range correlations exist due to Goldstone modes of a broken continu-

ous symmetry, as in superfluids or liquid crystals. A superfluid is characterized by a complex order parameter, whose phase  $\phi$  may vary across the system. The energy cost of such variations is governed by the Hamiltonian

$$\mathcal{H}[\phi] = \frac{K}{2} \int d^3\mathbf{x} (\nabla\phi)^2, \quad (3)$$

where the ‘‘phonon stiffness’’  $K$  is related to the superfluid density. In the Casimir geometry, the free energy of interaction resulting from thermal fluctuations of these modes has the form [11]

$$\delta\mathcal{F}(H) = -k_B T \times \frac{A}{H^2} \times \frac{\zeta(3)}{16\pi}. \quad (4)$$

Note that the result is universal, i.e. independent of the stiffness  $K$ . A similar result is obtained for the electromagnetic field at high temperatures  $k_B T \gg \hbar c/H$ , which is larger by a factor of two [12], reflecting the two polarizations of the normal modes.

Liquid Helium tends to wet most substrates, and the thickness of the wetting layer is controlled by the strength of the attractive forces that bind the film to the substrate [13]. The most important contribution for helium films comes from the van der Waals attraction. In the presence of a chemical potential cost of  $\delta\mu$  (e.g. coming from a gravitational potential difference), the energy of a film of thickness  $H$  is

$$\mathcal{H}_N = \frac{1}{2} \int d^3\mathbf{r} [\kappa_1(\nabla \cdot \mathbf{n})^2 + \kappa_2(\mathbf{n} \cdot \nabla \times \mathbf{n})^2 + \kappa_3(\mathbf{n} \times \nabla \times \mathbf{n})^2]. \quad (7)$$

Integrating over the nematic fluctuations leads to a free energy contribution

$$\delta\mathcal{E}_N = -k_B T \times \frac{A}{H^2} \times \frac{\zeta(3)}{16\pi} \left( \frac{\kappa_3}{\kappa_1} + \frac{\kappa_3}{\kappa_2} \right). \quad (8)$$

Note that the resulting force does depend on the relative strengths of the elastic coupling constants (reflecting the anisotropy of the system).

In a smectic liquid crystal, the molecules segregate into layers which are fluid like. The fluctuations of these layers from perfect stacking are described by a scalar deformation  $u(\mathbf{x}, z)$ , which is subject to a Hamiltonian

$$\mathcal{H}_S = \frac{1}{2} \int d^3\mathbf{r} \left[ B \left( \frac{\partial u}{\partial z} \right)^2 + \kappa (\nabla^2 u)^2 \right]. \quad (9)$$

The resulting interaction energy

$$\delta\mathcal{E}_S = -k_B T \times \frac{A}{H\lambda} \times \frac{\zeta(2)}{16\pi} \quad \text{with} \quad \lambda \equiv \sqrt{\frac{\kappa}{B}}, \quad (10)$$

falls off as  $1/H$ , reflecting the extreme anisotropy which has introduced an additional length scale  $\lambda$  into the problem.

Liquid crystal films provide an additional interesting feature in that their surfaces are typically more ordered

$$E(H) = A \left[ -\delta\mu H - \frac{C}{H^2} \right], \quad (5)$$

where  $C$  indicates the strength of the van-der Waals force. Minimizing this expression leads to a thickness

$$H = \left( \frac{2C}{\delta\mu} \right)^{1/3}. \quad (6)$$

However, when the helium film becomes superfluid, there is an additional attractive force due to Eq.(4), and there should thus be a jump in the film thickness. Actually, in the vicinity of the superfluid transition, there is another contribution to the force due to critical fluctuations, as in Eq.(2). Monitoring the thickness of the film may thus provide a test of these forces [14].

Liquid crystals exemplify anisotropic cases of correlated fluids due to broken symmetry, which again lead to fluctuation-induced forces [16,17,11]. They are also easily accessible, as experiments can be performed at room temperature and require no fine tuning to achieve criticality. The order parameter of a *nematic* liquid crystal is a director field  $\mathbf{n}(\mathbf{r})$ , characterizing the local preferred direction of the long axis of the molecules [15]. The energy cost of fluctuations of the nematic director  $\mathbf{n}(\mathbf{r})$  is given by [15]

than the bulk. This is because of the surface tension between the film and the surrounding gas which inhibits fluctuations of the molecules close to the surface [18]. Heat capacity experiments on free standing liquid crystal films near smectic-A (smA) to surface stabilized smectic-I (smI), and smA to surface stabilized smectic-B (smB) transitions have revealed a layer by layer ordering that starts at the surface and proceeds into the bulk [19,20]. The smB and smI phases are characterized by an additional bond-orientational (hexatic) order in the layers, while the molecules in smI are also tilted.

The wetting analogy suggests that, as in Eq.(6), the thickness of the hexatically ordered phases should grow with the reduced temperature  $t = (T - T_c)/T_c$  as  $t^{-\nu}$ , with  $\nu = 1/3$ . Here  $T_c$  is the bulk transition temperature, and we have assumed that the chemical potential difference is proportional to  $t$ . However, experiments find  $\nu \approx .32 \pm 0.01$  for the smA-smB transition [20], while at the smA-smI transition [19],  $\nu \approx 0.373 \pm 0.015$ . The difference between the two sets of experiments is rather surprising, as the underlying direct interactions (e.g. van der Waals), should be quite similar in the two cases. Is it possible that the fluctuation-induced forces are different in the two cases? The molecular tilt in smI provides a field that further pins the fluctuations of the hexatic

order at the surface. The effect of such a surface field on the force is explored in Ref. [21], leading to results consistent with the experimental observations.

## II. DISPERSION FORCES

In addition to his work on the force between plates, Casimir also realized [22] that the van der Waals and London [23] forces can also be understood on the same footing: The presence of the atoms modifies the fluctuations of the electromagnetic field, resulting in an attractive interaction. (For a modern perspective, see the discussion by Kleppner in Ref. [24].)

For example, let us consider two conducting spheres of volumes  $V_1 = 4\pi a_1^3/3$  and  $V_2 = 4\pi a_2^3/3$ , at a distance  $R$ . The fluctuation induced interaction is proportional to the product of the volumes, and thus on dimensional grounds we expect a potential

$$\mathcal{V}(R) = -k_B T \times \frac{V_1 V_2}{R^6} \times \Delta_T, \quad (11)$$

due to thermal fluctuations. Usually, the van der Waals interaction is obtained from the instantaneous induced dipoles on the spheres. However, it can be equivalently obtained by examining the electromagnetic fluctuations of the remaining space. When the fluctuations are of quantum origin, Eq.(11) is modified to

$$\mathcal{V}(R) = -\hbar c \times \frac{V_1 V_2}{R^7} \times \Delta_Q, \quad (12)$$

with  $\Delta_Q = 23/(4\pi)$  [22]. The cross-over between the two forms of the interaction occurs at a distance  $\lambda_T \sim \hbar c/k_B T$ .

Let us compare the above result with the more standard approach to calculating the London force between two neutral *atoms*: While the average dipole for each atom is zero, an instantaneous dipole fluctuation in one can induce a parallel instantaneous dipole on the other, leading to an attraction. Since the direct dipole-dipole interaction decays as  $1/R^3$ , the induced effect scales as the square, i.e.  $1/R^6$ . In this regards, it is similar to the result in Eq.(11), except that the characteristic energy is set by a typical atomic excitation energy of  $\hbar\omega_0$  rather than  $k_B T$ . The retardation effects are then obtained by taking into account the finite speed of light. We can imagine that for large enough distances when the signal goes from atom-1 to atom-2 to induce the dipole, and return to atom-1 to induce an attraction, it finds the dipole at atom-1 somewhat misaligned; resulting in a weaker attraction. The characteristic time for electron movements can be estimated from the frequency of the orbit as  $\tau = 2\pi/\omega_0$ . The crossover occurs when the travel time for the signal is comparable to this characteristic time, namely  $R/c \sim \tau$ . Hence, taking into account the retardation effect, the interaction is

$$\mathcal{V}_r(R) = -\hbar\omega_0 \times \frac{V_1 V_2}{R^6} \times f\left(\frac{R\omega_0}{c}\right). \quad (13)$$

The crossover function  $f(x)$  is a constant for  $x \rightarrow 0$  and vanishes as  $1/x$  for  $x \rightarrow \infty$ . It is clear that in the latter limit the dependence on  $\omega_0$  vanishes, and the Casimir-Polder result of Eq.(12) is recovered.

There are also interactions between spheres immersed in a critical fluid, which have been studied both analytically [25] and experimentally [26]. Surprisingly, the interaction does not have the same power-law forms as in Eq.(11); its exponents depending on the critical exponents, as well as boundary conditions [27].

Dispersion forces are not limited to particles in three dimensional space, but also occur for inclusions on films and membranes, the latter is of potential importance for understanding the interactions between proteins floating on a cell membrane. In addition to their structural role of forming the exterior frames of the cell and its interior organelles and vesicles, lipid bilayers act as the host and regulator of many biophysical and biochemical reactions [28,29]. Inter- and intra-cellular recognition and transport, adhesion, regulation of ion concentrations, and energy conversion, are but a few of the processes taking place at the membrane. These tasks are carried out by a variety of proteins, glycolipids, and other macromolecules that move through the many different lipids that make up the bilayer. It is thus essential to understand how inclusions affect the physical properties of the membrane, and how the membrane in turn contributes to the interactions between inclusions.

There are a number of different forces which act within membranes [30]: van der Waals interactions fall off with separation  $R$ , as  $1/R^6$  at long distances; the Coulomb interaction is strongly screened under physiological conditions (typical ion concentrations are a few millimolar, giving a screening length of less than  $10\text{\AA}$ ); hydration and structural forces are also short-ranged. There are additional interactions between inclusions which are mediated by the membrane; the inclusion disturbs the lipid bilayer and this disturbance propagates to neighboring inclusions (c.f. Refs. [29-33] and references therein). When macroscopic thermal fluctuations are unimportant (we refer to this case as  $T = 0$ ), the resulting interactions tend to be short-ranged, falling off exponentially with a characteristic length corresponding to the distance over which the lipid disturbance ‘‘heals.’’ For example, if in the region around an inclusion the membrane is forced to deviate from its preferred thickness ( $\sim 40\text{\AA}$ ), then the resulting disturbance decays exponentially with a length comparable to this thickness [33].

If the membrane is to mediate long-ranged interactions, then in the long-distance limit it should be possible to neglect the membrane thickness and details concerning lipid structure. In this limit, the membrane is well described by the elastic Hamiltonian [34],

$$\mathcal{H} = \int dS \left[ \sigma + \frac{\kappa}{2} H^2 + \bar{\kappa} K \right], \quad (14)$$

where  $dS$  is the surface area element, and  $H$ ,  $K$  are the mean and Gaussian curvatures respectively. The elastic properties of the surface are described by the tension  $\sigma$ , and the bending rigidities  $\kappa$  and  $\bar{\kappa}$ . A finite surface tension is the most important coupling in  $\mathcal{H}$  and dominates the bending terms at long wavelengths. This is the case for films on a frame, interfaces at short distances, and possibly closed membranes in the presence of osmotic pressure differences between their interior and exterior. On the other hand, for closed bilayers in the absence of osmotic stress, as well as for microemulsions, the surface tension is effectively zero [35–37]. In these cases, the energy cost of fluctuations is controlled by the rigidity terms. For simplicity we shall refer to surface tension dominated surfaces as films, and to rigidity controlled ones as membranes.

The long distance interactions between inclusions in a membrane were examined in Ref. [32]. It was shown that if the inclusions are asymmetric across the bilayer and impose a local curvature,  $\mathcal{H}$  gives rise to a repulsive ( $T = 0$ ) interaction that is long-ranged, falling off with distance as  $1/R^4$ . The energy scale of the interaction is set by  $\kappa$  and  $\bar{\kappa}$ . If thermal fluctuations of the membrane are included ( $T \neq 0$ ), on the other hand, there is a  $1/R^4$  interaction for *generic* inclusions, as long as the rigidity of

the inclusion differs from that of the ambient membrane [32]. In particular, if the inclusions are much stiffer than the membrane, the fluctuation-induced potential is

$$\mathcal{V}(R) = -k_B T \times \frac{A^2}{R^4} \times \frac{6}{\pi^2}, \quad (15)$$

where  $A$  is the area of each inclusion. (In this formula, the result in Ref. [32] has been corrected by a factor of  $1/2$  [38].) The interaction is attractive and independent of  $\kappa$  and  $\bar{\kappa}$ ; its energy scale set by  $k_B T$ . A generalization of this result that includes the quantum fluctuations of the membranes is given in Ref. [39].

The form of the interaction depends sensitively on the shapes of the inclusions, as demonstrated by the calculation of the fluctuation-induced interaction between rod-like objects [38]. The rods are assumed to be sufficiently rigid so that they do not deform coherently with the underlying membrane. They can thus only perform rigid translations and rotations while remaining attached to the surface. As a result, the fluctuations of the membrane are constrained, having to vanish at the boundaries of the rods. Consider the situation depicted in Fig. 1, with two rods of lengths  $L_1$  and  $L_2$  at a separation  $R \gg L_i$ . For fluctuating films ( $\sigma \neq 0$ ), there is an attractive fluctuation-induced interaction given by,

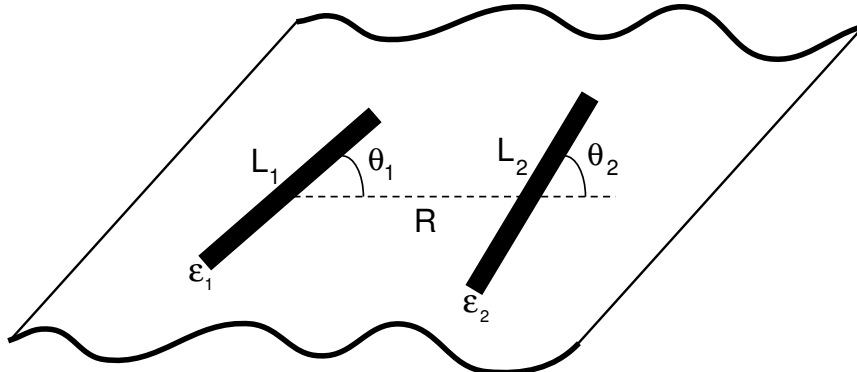


FIG. 1. Two rod-shaped inclusions embedded in a membrane. The rods are separated by a distance  $R$ . The  $i$ th rod has length  $L_i$ , width  $\epsilon_i$ , and makes an angle  $\theta_i$  with the line joining the centers of the two rods.

$$V_F^T(R, \theta_1, \theta_2) = -\frac{k_B T}{128} \times \frac{L_1^2 L_2^2}{R^4} \times \cos^2[\theta_1 + \theta_2] + O(1/R^6), \quad (16)$$

where  $\theta_1$  and  $\theta_2$  are the angles between the rods and the line adjoining their centers, as indicated in Fig. 1. This angular dependence is actually the *square* of that of a dipole-dipole interaction in two dimensions, with  $L_1$  and  $L_2$  as the dipole strengths. The fluctuation-induced interaction on a membrane ( $\sigma = 0$ ) is very similar and given by

$$V_M^T(R, \theta_1, \theta_2) = -\frac{k_B T}{128} \times \frac{L_1^2 L_2^2}{R^4} \times \cos^2[2(\theta_1 + \theta_2)] + O(1/R^6). \quad (17)$$

The orientational dependence is the *square* of a quadrupole–quadrupole interaction, with the unusual property of being minimized for both parallel and perpendicular orientations of the rods. Note that the strength of the interaction is the same in both cases. The above fluctuation-induced interactions decay less rapidly at large distances than van der

Waals forces and may play an important role in aligning asymmetric inclusions in biomembranes. Since orientational correlations are often easier to measure than forces, this result may also be useful as a probe of the fluctuation-induced interaction. Finally, this interaction could give rise to novel two-dimensional structures for collections of rodlike molecules. In particular, the resemblance of the orientational part of the interaction to dipolar forces suggests that a suitable way to minimize the energy of a collection of rods is to form them into chains. (If the rods are not colinear, the interactions cannot be minimized simultaneously.)

Finally, we note that these interactions cannot be obtained by adding two-body potentials on the rods: To find the orientational dependence of additive forces, let us consider an interaction  $U(|r_1 - r_2|)du_1du_2$ , between any two infinitesimal segments of two rods of length  $L$  at a distance  $R \gg L$ . Expanding  $|r_1 - r_2|$ , and integrating over the two rods, leads to the interaction

$$V(R, \theta_1, \theta_2) = L^2 U(R) + \frac{L^4}{6} \left( \frac{U'(R)}{R} + U''(R) \right) - \frac{L^4}{12} \left( \frac{U'(R)}{R} - U''(R) \right) (\cos 2\theta_1 + \cos 2\theta_2). \quad (18)$$

The angular dependence is now completely different, and minimized when the two rods are parallel to their axis of separation. Presumably both interactions are present for rods of finite thickness; the additive interaction is proportional to  $L^2(L\epsilon/R)^2$ , where  $\epsilon$  is the thickness. The previously calculated interactions are thus larger by a factor proportional to  $(R/\epsilon)^2$  and should dominate at large separations.

The effects of thermal fluctuations of membranes and films on embedded *directed semiflexible polymers* are examined in Ref. [40], using the path integral formulation of Ref. [11]. A semiflexible polymer with bending stiffness  $\kappa_p$  is rigid only at distances less than the bare persistence length  $\ell_p^0 = \kappa_p/k_B T$ . Upon embedding in a fluctuating surface, it is found that the induced interactions soften the rigidity of the polymer. While the reduction in persistence length  $\ell_p$  is not appreciable for polymers embedded in a film, there is a logarithmic reduction upon embedding in a membrane. The softening is more dramatic for two parallel rods, which due to their mutual attraction want to bend towards each other. This leads to an instability in the modes describing their relative *in-plane* fluctuations. The stiffness of the polymer prevents such instabilities only if the length of the polymer is less than a characteristic size  $L_p(R) \sim \ell_p^0 (R/\ell_p^0)^{3/4}$ , that depends on their separation  $R$  and is much lower than  $\ell_p^0$ .

The *out-of plane* fluctuations of the semiflexible polymers have a dramatic effect on their ‘‘Casimir’’ attraction. Consider two polymers embedded in the surface which are, on average, parallel to each other at separations  $a \ll R < L$ , where  $a$  is a microscopic length scale such as membrane thickness. The membrane and polymers have thermal fluctuations but are constrained to remain attached at all times. In the absence of *out-of plane* polymer fluctuations, there is a fluctuation-induced interaction that falls off as  $k_B T(L/R)$ . The *out-of plane* fluctuations actually screen out this interaction, resulting in a *short-ranged* attraction that can be approximately fitted to

$$\frac{F^\perp(R)}{L} = -\frac{k_B T}{2\pi} \times \frac{A}{R} \times \exp \left[ -b \left( \frac{R}{\lambda} \right)^\alpha \right], \quad (19)$$

where  $A_F = \pi^2/12$ ,  $A_M = 2.90514$ ,  $b_F = 3.32$ ,  $b_M = 4.17$ ,  $\alpha_F = 0.679$  and  $\alpha_M = 0.397$  are parameters obtained from numerical fits, corresponding to films and membranes respectively. The ‘‘screening’’ lengths that determine the range of the interactions are defined as  $\lambda_F = (\kappa_p/\sigma)^{1/3}$  for films and  $\lambda_M = \kappa_p/\kappa$  for membranes.

### III. PATH-INTEGRAL FORMULATION AND DEFORMED SURFACES

Most computations of Casimir forces are for simple geometries, e.g. between two parallel plates. It is natural to consider how these forces are modified by the roughness that is present in most ‘‘random’’ surfaces. There are a number of calculations that go beyond the simple planar geometry. For example, in Ref. [41] a multiple scattering approach is used to compute the interactions for arbitrary geometry in a perturbation series in the curvature. A phenomenological approach is introduced in Ref. [42] in which small deviations from plane parallel geometry are treated by using an additive summation of Casimir potentials. However, as demonstrated in the previous section, fluctuation induced forces are not additive, and additional steps are necessary to correct the result [42]. Another perturbative approach is introduced in Ref. [43], which is quite general, but suffers from rather cumbersome treatment of the boundary conditions. In Ref. [11], we introduced a path integral approach that made possible relatively simple computations of the fluctuation induced force. This approach has a number of advantages. First, different manifolds (with arbitrary intrinsic and embedding dimensions) in various correlated fluids can be treated in a similar fashion. Second, the boundary conditions are quite easily implemented, and the corrections can be computed perturbatively in the deformations.

Consider  $n$  manifolds embedded in a  $d$  dimensional correlated fluid, with an energy cost appropriately generalized from Eq.(3). The manifolds are described by the functions  $\mathbf{r}_\alpha(x_\alpha)$ , where  $x_\alpha$  is a  $D_\alpha$  dimensional internal coordinate ( $D_\alpha = 1$  for a polymer and  $D_\alpha = 2$  for

a membrane), while  $\mathbf{r}_\alpha$  indicates a position in the  $d$ -dimensional fluid. The fluctuation-induced interactions between the manifolds are obtained by integrating over all configurations of the field  $\phi$ , i.e.

$$\exp\left(-\frac{\mathcal{H}_{eff}[\mathbf{r}_\alpha(x_\alpha)]}{k_B T}\right) = \frac{1}{\mathcal{Z}_0} \int \mathcal{D}'\phi(\mathbf{r}) \exp(-\mathcal{H}_0[\phi]) . \quad (20)$$

$$\exp\left(-\frac{\mathcal{H}_{eff}}{k_B T}\right) = \frac{1}{\mathcal{Z}_0} \int \mathcal{D}\phi(\mathbf{r}) \prod_{\alpha=1}^n \mathcal{D}\psi_\alpha(x_\alpha) \exp\left(-\mathcal{H}_0[\phi] + i \int dx_\alpha \psi_\alpha(x_\alpha) \phi(\mathbf{r}_\alpha(x_\alpha))\right) , \quad (21)$$

where  $\psi_\alpha(x_\alpha)$  are the auxiliary fields defined on the  $n$  manifolds, acting as sources coupled to  $\phi$ . For the quadratic Hamiltonian of Eq.(3), it is easy to integrate over the field  $\phi$ , and obtain the long-range interactions between the sources as

$$\exp\left(-\frac{\mathcal{H}_{eff}}{k_B T}\right) = \int \prod_{\alpha=1}^n \mathcal{D}\psi_\alpha(x_\alpha) \exp(-\mathcal{H}_1[\psi_\alpha(x_\alpha)]) . \quad (22)$$

The action  $\mathcal{H}_1[\psi_\alpha(x_\alpha)]$  is a quadratic form for the  $n$  component field  $\Psi \equiv (\psi_1, \psi_2, \dots, \psi_n)$ , given by

$$\mathcal{H}_1[\Psi] \equiv \Psi M \Psi^T = \sum_{\alpha=1}^n \sum_{\beta=1}^n \int dx_\alpha dy_\beta \psi_\alpha(x_\alpha) G^d(\mathbf{r}_\alpha(x_\alpha) - \mathbf{r}_\beta(y_\beta)) \psi_\beta(y_\beta) , \quad (23)$$

where  $G^d(\mathbf{r}) \equiv \langle \phi(\mathbf{r}) \phi(0) \rangle_0$  is the two-point correlation function of the field  $\phi$  in free space. Finally, the effective interaction between the manifolds is obtained by performing the Gaussian integrations over the field  $\Psi$  as

$$\mathcal{H}_{eff}[\mathbf{r}_\alpha(x_\alpha)] = \frac{k_B T}{2} \ln \text{Det}(M[\mathbf{r}_\alpha(x_\alpha)]) . \quad (24)$$

The matrix  $M$  is a functional of  $\mathbf{r}_\alpha(x_\alpha)$  and its determinant is in general difficult to evaluate for arbitrary configurations. It is possible, however, to perturbatively calculate the corrections due to small deformations around simple base configurations. Consider two surfaces in  $d = 3$ , with average separation  $H$ . One plate has small deformations described by  $h(\mathbf{x})$ , i.e.  $\mathbf{r}_1(\mathbf{x}) = (x_1, x_2, 0)$ ,

Here  $\mathcal{D}'\phi(\mathbf{r})$  denotes the functional integral with the constraints imposed by the external manifolds, and  $\mathcal{Z}_0$  is the partition function for the unperturbed fluid. The boundary conditions ( $\phi(\mathbf{r}_\alpha(x_\alpha)) = 0$ , for  $\alpha = 1, 2, \dots, n$ ) are imposed by inserting delta functions. Using the integral representation of the delta function, Eq.(20) can be rewritten as

while  $\mathbf{r}_2(\mathbf{x}) = (x_1, x_2, H + h(\mathbf{x}))$ . The effective Hamiltonian can now be written as  $\mathcal{H}_{eff} = \mathcal{H}_{flat} + \mathcal{H}_{corr}$ , where  $\mathcal{H}_{flat}$  is the Casimir interaction for two flat plates, and  $\mathcal{H}_{corr}$  is the additional cost of deformations. For flat plates of area  $A$ , the interaction energy is

$$\frac{\mathcal{H}_{flat}}{A} = k_B T \frac{d^2 p}{(2\pi)^2} \ln\left(\frac{1}{2\alpha p}\right) - \frac{\zeta(3)}{16\pi} \frac{k_B T}{H^2} . \quad (25)$$

The first term in Eq.(25) is a contribution to the surface tension which depends on a lattice cutoff. The second term is the usual Casimir interaction, decaying as  $1/H^2$  and with a universal amplitude  $-\zeta(3)/16\pi \approx -0.02391$ . The energy cost of deformations is given by

$$\mathcal{H}_{corr} = -k_B T \times \frac{3\zeta(3)}{16\pi H^4} \int d^2 \mathbf{x} h^2(\mathbf{x}) + \frac{k_B T}{4} \int d^2 \mathbf{x} d^2 \mathbf{y} [h(\mathbf{x}) - h(\mathbf{y})]^2 \times \left\{ \frac{1}{8\pi^2 |\mathbf{x} - \mathbf{y}|^6} + \frac{1}{2\pi |\mathbf{x} - \mathbf{y}|^3 H^3} K_1\left(\frac{|\mathbf{x} - \mathbf{y}|}{H}\right) + \frac{1}{H^6} \left[ K_1\left(\frac{|\mathbf{x} - \mathbf{y}|}{H}\right) \right]^2 + \frac{1}{H^6} \left[ K_2\left(\frac{|\mathbf{x} - \mathbf{y}|}{H}\right) \right]^2 \right\} , \quad (26)$$

with two kernel functions defined by

$$K_1(t) \equiv \int_0^\infty du \frac{u^2}{2\pi(e^{2u}-1)} J_0(tu) , \quad (27)$$

$$K_2(t) \equiv \int_0^\infty du \frac{u^2 e^u}{2\pi(e^{2u}-1)} J_0(tu) . \quad (28)$$

The first term in Eq.(26) represents an instability to deformations that is related to the attraction between the plates. Remarkably, this term can be obtained intuitively by replacing  $1/H^2$  with  $1/(H + h(\mathbf{x}))^2$  in Eq.(25) and

averaging over the position  $\mathbf{x}$ . The second term represents long-range interactions between the deformations, induced by the fluctuations of the field. The first term in the curly brackets is the conformation energy of the deformed surface in the absence of the second plane, and is independent of  $H$ . The remaining terms represent correlations due to the presence of second plane. Both  $K_1(t)$  and  $K_2(t)$  approach a constant as  $t \rightarrow 0$ . As  $t \rightarrow \infty$ ,  $K_1(t) \sim 1/t^3$ , while  $K_2(t) \sim \exp(-bt)$ , with  $b \approx 3.3$ . The large  $t$  behaviors of  $K_1(t)$  and  $K_2(t)$  determine the

long-range interactions between height fluctuations.

Eq.(26) can be used to calculate the Casimir force between a flat and a quenched rough surface. Many solid surfaces produced by rapid growth or deposition processes are characterized by self-similar fluctuations [44]. The fluctuations of a self-affine surface grow as

$$\overline{[h(\mathbf{x}) - h(\mathbf{y})]^2} = A_S |\mathbf{x} - \mathbf{y}|^{2\zeta_S}, \quad (29)$$

where the overbar denotes quenched average, and  $\zeta_S$  is a characteristic roughness exponent. Using Eq.(29) we can take the average of the  $H$  dependent terms in  $\mathcal{H}_{eff}$ , to

$$C_1 = \int_{\frac{a}{H}}^{\frac{L}{H}} \{-t^{2\zeta_S-2} K_1(t) + 2\pi t^{2\zeta_S+1} [K_1(t)]^2 + 2\pi t^{2\zeta_S+1} [K_2(t)]^2\} dt, \quad (31)$$

and does weakly depend on the ratio  $L/H$ , but since the functions  $K_1$  and  $K_2$  decay rapidly at large distance, it is quite insensitive to  $L$  as long as  $L \gg H$ . As long as  $L \gg H \gg \Delta H$ , the interactions in Eq.(30) are arranged in order of increasing strength. The largest effect of randomness is to increase the Casimir attraction by an amount proportional to  $(\Delta H/H)^2$ . There is also another correction term, of the opposite sign, that decays as  $1/H^{4-2\zeta_S}$ , and in principle can be used to indirectly measure the roughness exponent  $\zeta_S$ . In Eq.(29), if all lengths are measured in units of an atomic scale  $a_0$  (e.g. the diameter of a surface atom),  $A_S$  becomes dimensionless. Using a reasonable set of parameters:  $\zeta_S \approx 0.35$ ,  $a_0 \approx 5\text{\AA}$ ,  $A_S \approx 1$  and  $L \approx 300\text{\AA}$ , we estimate that for surfaces of 1mm size, and 100 $\text{\AA}$  apart, the forces generated by the three terms in Eq.(30) are  $1.9 \times 10^{-4}$ ,  $4.9 \times 10^{-5}$ , and  $3.7 \times 10^{-6}\text{N}$  respectively, (with appropriate lower cutoff  $\sim 20\text{\AA}$ ), which is measurable with the current force apparatus [5].

The calculation of the effective partition function in Eq.(21) is easily extended to four dimensional space-time. In a relativistic theory, the space and time coordinates are related by Poincaré symmetries, and the action for a free scalar field takes the simple form

$$S = \frac{1}{2} \int d^4X \partial_\mu \phi(X) \partial_\mu \phi(X), \quad (32)$$

where summation over  $\mu = 0, \dots, 3$  is implicit. Following a Wick rotation, imaginary time appears as another coordinate  $X_4 = ict$  in the 4-dimensional space-time. In a path integral formulation, the different configurations of the field  $\phi$  are now weighted by  $\exp[-S/\hbar]$ . The boundary conditions on the field are implemented by inserting delta-functions as before. However, because of the symmetry between space and time coordinates, we are now at liberty to impose the boundary condition on a manifold  $\vec{r}(\mathbf{x}, t)$ , i.e. we can treat deformations in space and time on the same footing. This allows us to address the problem of the dynamic Casimir effect, which is the topic of the next section.

obtain a free energy per unit area

$$\mathcal{F}(H) = -\frac{k_B T \zeta(3)}{H^2 16\pi} - \frac{k_B T A_S L^{2\zeta_S} 3\zeta(3)}{H^4 16\pi} + \frac{k_B T A_S C_1}{H^{4-2\zeta_S} 4}, \quad (30)$$

where  $L$  the extent (upper cutoff) of the self-affine structure, satisfying  $\Delta H \equiv A_S^{\frac{1}{\zeta_S}} L^{\zeta_S} \ll H$ . (This is the condition that the total width due to roughness,  $\Delta H$  is less than the average separation  $H$ , so that the plates are not in contact.) The coefficient  $C_1$  in Eq.(30) is given by

#### IV. THE DYNAMIC CASIMIR EFFECT

Although less well known than its static counterpart, the dynamical Casimir effect, describing the force and radiation from moving mirrors has also garnered much attention [45–51]. This is partly due to connections to Hawking and Unruh effects (radiation from black holes and accelerating bodies, respectively), suggesting a deeper link between quantum mechanics, relativity, and cosmology [52].

The creation of photons by moving mirrors was first obtained by Moore [45] for a 1 dimensional cavity. Fulling and Davis [46] demonstrated that there is a corresponding force, even for a single mirror, which depends on the third time derivative of its displacement. These computations take advantage of conformal symmetries of the 1+1 dimensional space time, and can not be easily generalized to higher dimension. Furthermore, the calculated force has causality problems reminiscent of the radiation reaction forces in classical electron theory [47]. It has been shown that this problem is an artifact of the unphysical assumption of perfect reflectivity of the mirror, and can be resolved by considering realistic frequency dependent reflection and transmission from the mirror [47].

Another approach to the problem starts with the fluctuations in the force on a single plate. The fluctuation-dissipation theorem is then used to obtain the mechanical response function [48], whose imaginary part is related to the dissipation. This method does not have any causality problems, and can also be extended to higher dimensions. (The force in 1+3 dimensional space-time depends on the fifth power of the motional frequency.) The emission of photons by a perfect cavity, and the observability of this energy, has been studied by different approaches [49–51]. The most promising candidate is the resonant production of photons when the mirrors vibrate at the optical resonance frequency of the cavity [52]. A review, and more extensive references are found in Ref. [53]. More recently, the radiation due to vacuum fluctuations of a collapsing

bubble has been proposed as a possible explanation for the intriguing phenomenon of sonoluminescence [54,55].

Here, we follow the path integral formulation [56], outlined in the previous section, for the problem of perfectly reflecting mirrors that undergo arbitrary dynamic deformations. We apply the path integral quantization formalism to a scalar field  $\phi$  with the action in Eq.(32). In principle, we should use the electromagnetic vector potential  $A_\mu(X)$ , but requirements of gauge fixing complicate the calculations, while the final results only change by a numerical prefactor. (We have explicitly checked that we reproduce the known answer for flat plates by this method.) We would like to quantize the field subject to the constraints of its vanishing on a set of  $n$  manifolds (objects) defined by  $X = X_\alpha(y_\alpha)$ , where  $y_\alpha$  parametrize the  $\alpha$ th manifold. We implement the constraints using delta functions, and write the partition function as

$$\mathcal{Z} = \int \mathcal{D}\phi(X) \prod_{\alpha=1}^n \prod_{y_\alpha} \delta(\phi(X_\alpha(y_\alpha))) \exp \left\{ -\frac{S[\phi]}{\hbar} \right\}. \quad (33)$$

$$S_{\text{eff}} = \frac{\hbar c}{2} \int \frac{d\omega d^2\mathbf{q}}{(2\pi)^3} [A_+(q, \omega) (|h_1(\mathbf{q}, \omega)|^2 + |h_2(\mathbf{q}, \omega)|^2) - A_-(q, \omega) (h_1(\mathbf{q}, \omega)h_2(-\mathbf{q}, -\omega) + h_1(-\mathbf{q}, -\omega)h_2(\mathbf{q}, \omega))] + O(\hbar^3). \quad (34)$$

The kernels  $A_\pm(q, \omega)$ , that are closely related to the mechanical response of the system (see below), are functions of the separation  $H$ , but depend on  $\mathbf{q}$  and  $\omega$  only through the combination  $Q^2 = q^2 - \omega^2/c^2$ . The closed forms for these kernels involve cumbersome integrals, and are not very illuminating. Instead of exhibiting these formulas, we shall describe their behavior in various regions of the parameter space. In the limit  $H \rightarrow \infty$ ,  $A_\pm^\infty(q, \omega) = 0$ , and

$$A_+^\infty(q, \omega) = \begin{cases} -\frac{1}{360\pi^2 c^5} (c^2 q^2 - \omega^2)^{5/2} & \text{for } \omega < cq, \\ i \frac{\text{sgn}(\omega)}{360\pi^2 c^5} (\omega^2 - c^2 q^2)^{5/2} & \text{for } \omega > cq, \end{cases} \quad (35)$$

where  $\text{sgn}(\omega)$  is the sign function. While the effective action is real for  $Q^2 > 0$ , it becomes purely imaginary for  $Q^2 < 0$ . The latter signifies dissipation of energy [48], presumably by generation of photons [51]. It agrees precisely with the results obtained previously [48] for the special case of flat mirrors ( $\mathbf{q} = 0$ ). (Note that dissipation is already present for a single mirror.)

The delta functions are next represented by integrals over Lagrange multiplier fields. Performing the Gaussian integrations over  $\phi(X)$  then leads to an effective action for the Lagrange multipliers which is again Gaussian [11]. Evaluating  $\mathcal{Z}$  is thus reduced to calculating the logarithm of the determinant of a kernel. Since the Lagrange multipliers are defined on a set of manifolds with nontrivial geometry, this calculation is generally complicated. To be specific, we focus on two parallel 2d plates embedded in 3+1 space-time, and separated by an average distance  $H$  along the  $x_3$ -direction. Deformations of the plates are parametrized by the height functions  $h_1(\mathbf{x}, t)$  and  $h_2(\mathbf{x}, t)$ , where  $\mathbf{x} \equiv (x_1, x_2)$  denotes the two lateral space coordinates while  $t$  is the time variable. Following Ref. [11],  $\ln \mathcal{Z}$  is calculated by a perturbative series in powers of the height functions. The resulting expression for the effective action (in real time), defined by  $S_{\text{eff}} \equiv -i\hbar \ln \mathcal{Z}$ , after eliminating  $h$  independent terms, is

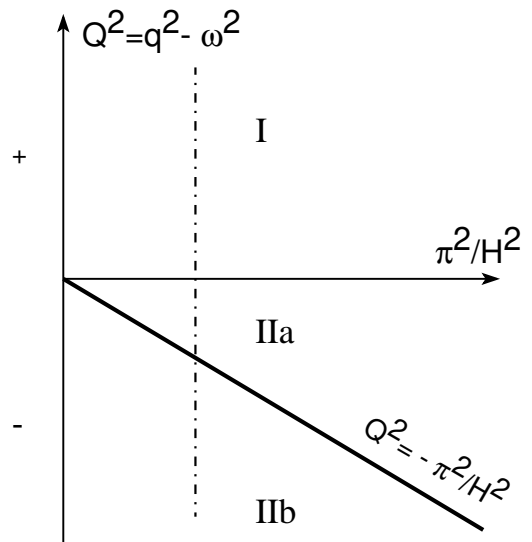


FIG. 2. Different regions of the  $(\mathbf{q}, \omega)$  plane.

In the presence of a second plate (i.e. for finite  $H$ ), the parameter space of the kernels subdivides into three different regions as depicted in Fig. 2. In region I ( $Q^2 > 0$  for any  $H$ ), the kernels are finite and real, and hence there is no dissipation. In region IIa where  $-\pi^2/H^2 \leq Q^2 < 0$ , the  $H$ -independent part of  $A_+$  is imaginary, while the  $H$ -dependent parts of both kernels are real and finite. (This is also the case at the boundary  $Q^2 = -\pi^2/H^2$ .) The dissipation in this regime is simply the sum of what would have been observed if the individual plates were decoupled, and unrelated to the separation  $H$ . By con-

trast, in region IIb where  $Q^2 < -\pi^2/H^2$ , both kernels diverge with infinite real and imaginary parts [57]. This  $H$ -dependent divergence extends all the way to the negative  $Q^2$  axis, where it is switched off by a  $1/H^5$  prefactor.

As a concrete example, let us examine the lateral vibration of plates with fixed roughness, such as two corrugated mirrors. The motion of the plates enters through the time dependencies  $h_1(\mathbf{x}, t) = h_1(\mathbf{x} - \mathbf{r}(t))$  and  $h_2(\mathbf{x}, t) = h_2(\mathbf{x})$ ; i.e. the first plate undergoes lat-

$$\chi_{ij}(\omega) = \hbar c \int \frac{d^2q}{(2\pi)^2} q_i q_j \left\{ [A_+(q, \omega) - A_+(q, 0)] |h_1(\mathbf{q})|^2 + \frac{1}{2} A_-(q, 0) (h_1(\mathbf{q})h_2(-\mathbf{q}) + h_1(-\mathbf{q})h_2(\mathbf{q})) \right\}, \quad (37)$$

and there is a residual force

$$f_i^0(\omega) = -\frac{\hbar c}{2} 2\pi\delta(\omega) \int \frac{d^2q}{(2\pi)^2} i q_i A_-(q, 0) (h_1(\mathbf{q})h_2(-\mathbf{q}) - h_1(-\mathbf{q})h_2(\mathbf{q})). \quad (38)$$

Let us now consider a corrugated plate with a deformation  $h_1(\mathbf{x}) = d \cos(\mathbf{k} \cdot \mathbf{x})$ . From the frequency-wavevector dependence of the mechanical response function in Eq.(37), we extract a plethora of interesting results, some of which we list below:

**1. Mass corrections:** For a single plate ( $H \rightarrow \infty$ ), we can easily calculate the response tensor using the explicit formulas in Eq.(35). In the limit of  $\omega \ll ck$ , expanding the result in powers of  $\omega$  gives  $\chi_{ij} = \delta m_{ij} \omega^2 + O(\omega^4)$ , where  $\delta m_{ij} = A \hbar d^2 k^3 k_i k_j / (288 \pi^2 c)$ , can be regarded as corrections to the mass of the plate. (Cut-off dependent mass corrections also appear, as in Ref. [53].) Note that these mass corrections are *anisotropic* with

$$\begin{aligned} \delta m_{\parallel} &= \frac{1}{288 \pi^2} \frac{\hbar}{c} A d^2 k^5, \\ \delta m_{\perp} &= 0. \end{aligned} \quad (39)$$

Parallel and perpendicular components are defined with respect to  $\mathbf{k}$ , and  $A$  denotes the area of the plates. The mass correction is inherently very small: For a macroscopic sample with  $d \approx \lambda = 2\pi/k \approx 1\text{mm}$ , density  $\approx 15\text{gr/cm}^3$ , and thickness  $t \approx 1\text{mm}$ , we find  $\delta m/m \sim 10^{-34}$ . Even for deformations of a microscopic sample of atomic dimensions (close to the limits of the applicability of our continuum representations of the boundaries),  $\delta m/m$  can only be reduced to around  $10^{-10}$ . With the second plate at a separation  $H$ , the mass renormalization becomes a function of both  $k$  and  $H$ , with a crossover from the single plate behavior for  $kH \sim 1$ . In the limit of  $kH \ll 1$ , we obtain  $\delta m_{\parallel} = \hbar A B k^2 d^2 / 48 c H^3$  and  $\delta m_{\perp} = 0$ , with  $B = -0.453$ . Compared to the single plate, there is an enhancement by a factor of  $(kH)^{-3}$  in  $\delta m_{\parallel}$ . While the actual changes in mass are immeasurably small, the hope is that its *anisotropy* may be more accessible, say by comparing oscillation frequencies of a plate in two orthogonal directions.

**2. Dissipation:** For  $\omega \gg ck$  the response function is imaginary, and we define a frequency dependent effective

eral motion described by  $\mathbf{r}(t)$ , while the second plate is stationary. The lateral force exerted on the first plate is obtained from  $f_i(t) = \delta S_{\text{eff}} / \delta r_i(t)$ . Within linear response, it is given by

$$f_i(\omega) = \chi_{ij}(\omega) r_j(\omega) + f_i^0(\omega), \quad (36)$$

where the ‘‘mechanical response tensor’’ is

shear viscosity by  $\chi_{ij}(\omega) = -i\omega\eta_{ij}(\omega)$ . This viscosity is also anisotropic, with

$$\begin{aligned} \eta_{\parallel}(\omega) &= \frac{1}{720 \pi^2} \frac{\hbar}{c^4} A d^2 k^2 \omega^4, \\ \eta_{\perp}(\omega) &= 0. \end{aligned} \quad (40)$$

Note that the dissipation is proportional to the fifth time derivative of displacement, and there is no dissipation for a uniformly accelerating plate. However, a freely oscillating plate will undergo a damping of its motion. The characteristic decay time for a plate of mass  $M$  is  $\tau \approx 2M/\eta$ . For the macroscopic plate of the previous paragraph, vibrating at a frequency of  $\omega \approx 2ck$  (in the  $10^{12}\text{Hz}$  range), the decay time is enormous,  $\tau \sim 10^{18}\text{s}$ . However, since the decay time scales as the fifth power of the dimension, it can be reduced to  $10^{-12}\text{s}$ , for plates of order of 10 atoms. However, the required frequencies in this case (in the  $10^{18}\text{Hz}$  range) are very large. Also note that for the linearized forms to remain valid in this high frequency regime, we must require very small amplitudes, so that the typical velocities involved  $v \sim r_0\omega$ , are smaller than the speed of light. The effective dissipation in region IIa of Fig. 2 is simply the sum of those due to individual plates, and contains no  $H$  dependence.

**3. Resonant Emission:** The cavity formed between the two plates supports continuous spectrum of normal modes for frequencies  $\omega^2 > c^2(k^2 + \pi^2/H^2)$ . We find that both real and imaginary parts of  $A_{\pm}(k, \omega)$ , diverge in this regime which we interpret as resonant dissipation due to excitation of photons in the cavity. Resonant dissipation has profound consequences for motion of plates. It implies that due to quantum fluctuations of vacuum, *components of motion with frequencies in the range of divergences cannot be generated by any finite external force!* The imaginary parts of the kernels are proportional to the total number of excited photons [51]. Exciting these degrees of motion must be accompanied by the generation of an infinite number of photons; requiring an infinite amount of energy, and thus impossible. However,

as pointed out in Ref. [51], the divergence is rounded off by assuming finite reflectivity and transmissivity for the mirrors. Hence, in practice, the restriction is softened and controlled by the degree of ideality of the mirrors in the frequency region of interest.

Related effects have been reported in the literature for 1+1 dimensions [49–52], but occurring at a *discrete* set of frequencies  $\omega_n = n\pi c/H$  with integer  $n \geq 2$ . These resonances occur when the frequency of the external perturbation matches the natural normal modes of the cavity, thus exciting quanta of such modes. In one space dimension, such modes are characterized by a discrete set of wavevectors that are integer multiples of  $\pi/H$ . The restriction to  $n \geq 2$  is a consequence of quantum electrodynamics being a ‘free’ theory (quadratic action): only two-photon states can be excited subject to conservation of energy. Thus the sum of the frequencies of the two photons should add up to the external frequency [51]. In higher dimensions, the appropriate parameter is the combination  $\omega^2/c^2 - q^2$ . From the perspective of the excited photons, conservation of momentum requires that their two momenta add up to  $q$ , while energy conservation restricts the sum of their frequencies to  $\omega$ . The in-plane momentum  $q$ , introduce a continuous degree of freedom: the resonance condition can now be satisfied for a continuous spectrum, in analogy with optical resonators. In Ref. [51], the lowest resonance frequency is found to be  $2\pi c/H$  which seems to contradict our prediction. However, the absence of  $\omega_1 = \pi c/H$  in 1+1 D is due to a vanishing prefactor [51], which is also present in our calculations. However, in exploring the continuous frequency spectrum in higher dimensions, this single point is easily bypassed, and there is a divergence for all frequencies satisfying  $\omega^2/c^2 > q^2 + \pi^2/H^2$ , where the inequality holds in its strict sense.

**4. “Josephson”-like Effects:** The constant term in Eq.(38) is sensitive to the shapes of the plates. For two plates corrugated at the same wavelength, with deformations  $h_1(\mathbf{x}) = d_1 \cos(\mathbf{k} \cdot \mathbf{x})$  and  $h_2(\mathbf{x}) = d_2 \cos(\mathbf{k} \cdot \mathbf{x} + \alpha)$ , there is a (time independent) lateral force

$$\mathbf{F}_{dc} = \frac{\hbar c A}{2} A_-(k, 0) \mathbf{k} d_1 d_2 \sin \alpha, \quad (41)$$

which tends to keep the plates 180 degrees out of phase, i.e. mirror symmetric with respect to their mid-plane. The dependence on the sine of the phase mismatch is reminiscent of to the DC Josephson current in superconductor junctions, the force playing a role analogous to the current in SIS junctions. There is also an analog for the AC Josephson effect, with velocity (the variable conjugate to force) playing the role of voltage: Consider two corrugated plates separated at a distance  $H$ , described by  $h_1(\mathbf{x}, t) = d_1 \cos[\mathbf{k} \cdot (\mathbf{x} - \mathbf{r}(t))]$  and  $h_2(\mathbf{x}, t) = d_2 \cos[\mathbf{k} \cdot \mathbf{x}]$ . The resulting force at a constant velocity ( $\mathbf{r}(t) = \mathbf{v} t$ ),

$$\mathbf{F}_{ac} = \frac{\hbar c A}{2} A_-(k, 0) \mathbf{k} d_1 d_2 \sin[(\mathbf{k} \cdot \mathbf{v}) t], \quad (42)$$

oscillates at a frequency  $\omega = \mathbf{k} \cdot \mathbf{v}$ . Actually both effects are a consequence of the attractive nature of the Casimir force. It would be difficult to separate them from similar forces resulting from say, van der Waals attractions.

**5. Surface Tension Corrections:** Finally, let us consider the capillary waves on the surface of mercury, with a conducting plate placed at a separation  $H$  above the surface. The low frequency–wavevector expansion of the kernel due to quantum fluctuations in the intervening vacuum, starts with quadratic forms  $q^2$  and  $\omega^2$ . These terms result in corrections to the (surface) mass density by  $\delta\rho = \hbar B/48cH^3$ , and to the surface tension by  $\delta\sigma = \hbar cB/48H^3$ . The latter correction is larger by a factor of  $(c/c_s)^2$ , and changes the velocity  $c_s$ , of capillary waves by  $\delta c_s/c_s^0 = \hbar cB/96\sigma H^3$ , where  $\sigma$  is the bare surface tension of mercury. Taking  $H \sim 1\text{mm}$  and  $\sigma \sim 500$  dynes/cm, we find another very small correction of  $\delta c_s/c_s^0 \sim 10^{-19}$ .

## ACKNOWLEDGMENTS

MK is supported by the NSF grant DMR-93-03667, and has benefitted from collaborations on these problems with H. Li, M. Goulian, and M. Lyra. RG acknowledges many helpful discussions with M.R.H. Khajehpour, B. Mashhoon, S. Randjbar-Daemi, and Y. Sobouti, and support from the Institute for Advanced Studies in Basic Sciences, Gava Zang, Zanjan, Iran.

- 
- [1] H.B.G. Casimir, Proc. K. Ned. Akad. Wet. **51**, 793 (1948).
  - [2] I.I. Abricossova and B.V. Deryaguin, Dokl. Akad. Nauk. SSSR **90**, 1055 (1953).
  - [3] M.J. Sparnaay, Physica **24**, 751 (1958).
  - [4] See, e.g. J.N. Israelachvili and P.M. McGuigan, Science **241**, 6546 (1990).
  - [5] S.K. Lamoreaux, Phys. Rev. Lett. **78**, 5 (1997).
  - [6] M. Krech, *The Casimir Effect in Critical Systems* (World Scientific, Singapore, 1994).
  - [7] M.E. Fisher and P.-G. de Gennes, C. R. Acad. Sci. Ser. B **287**, 207 (1978); V. Privman and M.E. Fisher, Phys. Rev. B **30**, 322 (1984).
  - [8] H.W.J. Blöte, J.L. Cardy, and M.P. Nightingale, Phys. Rev. Lett. **56**, 742 (1986).
  - [9] M.P. Nightingale and J.O. Indekeu, Phys. Rev. Lett. **54**, 1824 (1985).
  - [10] M. Krech and S. Dietrich, Phys. Rev. Lett. **66**, 345 (1991).
  - [11] H. Li and M. Kardar, Phys. Rev. Lett. **67**, 3275 (1991); Phys. Rev. A **46**, 6490 (1992).
  - [12] J. Schwinger, L.L. DeRaad, and K.A. Milton, Ann. Phys. (N.Y.) **115**, 1 (1978).

- [13] For a review see, e.g., S. Dietrich, in *Phase Transitions and Critical Phenomena*, edited by C. Domb and J.L. Lebowitz (Academic, New York, 1988), vol.12.
- [14] Privately communicated proposal by Moses Chen, Penn. State Univ. (1996).
- [15] P.-G. de Gennes, *The physics of Liquid Crystals* (Oxford Univ. Press, Oxford, 1974).
- [16] L.V. Mikheev, Sov. Phys. JEPT **69**, 358 (1989).
- [17] A. Ajdari, L. Peliti and J. Prost, Phys. Rev. Lett. **66**, 1481 (1991).
- [18] J.V. Selinger and D. Nelson, Phys. Rev. A **37**, 1736 (1988); R. Holyst, D.J. Tweet and L.B. Sorensen, Phys. Rev. Lett. **65**, 2153 (1990).
- [19] B.D. Swanson, H. Straigler, D.J. Tweet and L.B. Sorensen, Phys. Rev. Lett. **62**, 909 (1989).
- [20] T. Stoebe, R. Geer, C.C. Huang and J.W. Goodby, Phys. Rev. Lett. **69**, 2090 (1992).
- [21] M.L. Lyra, M. Kardar, and N. F. Svaiter, Phys. Rev. E **47**, 3456 (1993).
- [22] H.B.G. Casimir and D. Polder, Phys. Rev. **73**, 360 (1948).
- [23] F. London, Z. Phys. Chem. B **11**, 222 (1930).
- [24] D. Kleppner, Physics Today, October 1990, page 9.
- [25] P.-G. de Gennes, C. R. Acad. Sci. Paris II **292**, 701 (1981).
- [26] D. Beysens, J.-M. Petit, T. Narayan, A. Kumar, and M.L. Broide, Ber. Bunsen-Ges. Phys. Chem. **98**, 382 (1984).
- [27] T.W. Burkhardt and E. Eisenreigler, Phys. Rev. Lett. **74**, 3189 (1995).
- [28] B. Alberts, J. Lewis, M. Raff, K. Roberts and J.D. Watson, *Molecular Biology of the Cell*, Garland, New York 1994.
- [29] R.B. Gennis, *Biomembranes, Molecular Structure and Function*, Springer-Verlag, New York 1989.
- [30] J. Israelachvili, *Intermolecular and Surface Forces* (Academic Press, San Diego 1992).
- [31] O.G. Mouritsen and M. Bloom, Annu. Rev. Biophys. Biomol. Struct. **22**, 145 (1993).
- [32] M. Goulian, R. Bruinsma, and P. Pincus, Europhys. Lett. **22**, 145 (1993); Erratum in Europhys. Lett. **23**, 155 (1993).
- [33] N. Dan, P. Pincus, and S.A. Safran, Langmuir **9**, 2768 (1993).
- [34] P.B. Canham, J. Theor. Biol. **26**, 61 (1970); W. Helfrich, Z. Naturforsch. **28c**, 693 (1973).
- [35] P.G. de Gennes and C. Taupin, J. Phys. Chem. **86**, 2294 (1982).
- [36] F. Brochard and J.F. Lennon, J. de Phys. **36**, 1035 (1975).
- [37] F. David and S. Leibler, J. de Phys. II **1**, 959 (1991).
- [38] R. Golestanian, M. Goulian, and M. Kardar, Europhys. Lett. **33**, 241 (1996); Phys. Rev. E **54**, 6725 (1996).
- [39] E. D'Hoker, P. Sikivie, and Y. Kanev, Phys. Lett. B **347**, 56 (1995).
- [40] R. Golestanian, Europhys. Lett. **36**, 557 (1996).
- [41] R. Balian and B. Duplantier, Annals of Phys. **112**, 165 (1978).
- [42] M. Bordag, G.L. Klimchitskaya, and V.M. Mostepanenko, Int. J. Mod. Phys. A **10**, 2661 (1995).
- [43] L.H. Ford and A. Vilenkin, Phys. Rev. D **25**, 2569 (1982).
- [44] M. Kardar, in *Proceedings of the 4th International Conference on Surface X-Ray and Neutron Scattering*, eds. G.p. Felcher and H. You, Physica B **221**, 60 (1996).
- [45] G.T. Moore, J. Math. Phys. **11**, 2679 (1970).
- [46] S.A. Fulling, and P.C.W. Davies, Proc. R. Soc. A **348**, 393 (1976).
- [47] M.-T. Jaekel, and S. Reynaud, Phys. Lett. A **167**, 227 (1992).
- [48] P.A. Maia Neto, and S. Reynaud, Phys. Rev. A **47**, 1639 (1993).
- [49] G. Calucci, J. Phys. A: Math. Gen. **25**, 3873 (1992); C.K. Law, Phys. Rev. A **49**, 433 (1994); V.V. Dodonov, Phys. Lett. A **207**, 126 (1995).
- [50] O. Meplan and C. Gignoux, Phys. Rev. Lett. **76**, 408 (1996).
- [51] A. Lambrecht, M.-T. Jaekel, and S. Reynaud, Phys. Rev. Lett. **77**, 615 (1996).
- [52] P. Davis, Nature **382**, 761 (1996).
- [53] G. Barton and C. Eberlein, Ann. Phys. (N.Y.) **227**, 222 (1993).
- [54] C. Eberlein, Phys. Rev. Lett. **76**, 3842 (1996); Phys. Rev. A **53**, 2772 (1996).
- [55] P. Knight, Nature **381**, 736 (1996).
- [56] R. Golestanian and M. Kardar, Phys. Rev. Lett. **78**, 3421 (1997).
- [57] The divergence of kernels in IIb comes from integrations over space-time. Given a cut-off  $L$  in plate size, and an associated cutoff  $L/c$  in time, the kernels diverge as  $\exp[(K-2)L/H]/[K(L/H)^3]$ , with  $K = 2QH/\pi$ . Some care is necessary in the order of limits for  $(L, H) \rightarrow \infty$ .